

# ON THE SHIELDING OF ENGINE NOISE BY AN AIRCRAFT WING

L. M. B. C. Campos, F. J. P. Lau

\*Secção de Mecânica Aeroespacial, ISR, Instituto Superior Técnico, 1049-001, Lisboa Codex, Portugal

**Keywords:** Noise, Wing, Shielding, Huyghens' Principle

## Abstract

The shielding of noise radiation by interposing a flat plate between the observer and source is considered, using Huyghens' principle to replace the real source by a virtual source distribution outside the plate. A shielding factor is introduced as the ratio of the acoustic pressure received by the observer in the presence of an obstacle (*i.e.* the plate) and in its absence (*i.e.* in free space). The shielding factor is calculated for arbitrary observer and source positions relative to the plate, and is simplified for observer in the far-field and source in the near-field, and then for both in the far-field. The shielding factor is plotted as a function of source position relative to the plate, for an observer in the far-field and a range of frequencies in the audible spectrum. This simulates the effect of engine position relative to the wing, on fly-over noise, for an airliner with overwing mounted engines, over the noise spectrum of relevance to airport noise.

## 1 Introduction

The effect of interfaces, obstacles and slits on the propagation of sound can be studied by several techniques, including (*i*) diffraction, (*ii*) scattering, (*iii*) Fourier and (*iv*) Fresnel methods. The diffraction method (*i*) in exact form solves the acoustic wave equation with boundary conditions, *e.g.* the Sommerfeld<sup>1</sup> edge problem<sup>2</sup>; the Wiener-Hopf technique<sup>3</sup> is used for similar diffraction problems, *e.g.* a splitter plate<sup>4</sup> or

three semi-infinite plates<sup>5</sup>. Further extensions include diffraction by a thick plate<sup>6</sup>, a periodic array<sup>7</sup>, a cylinder<sup>8</sup> and a torus<sup>9</sup>. The scattering method (*ii*) specifies reflection and transmission coefficients<sup>10</sup>, *e.g.* for tube junctions<sup>11,12</sup>, impedance<sup>13</sup> and shear<sup>14,15</sup> layers, including cases of multiple scattering<sup>16,17</sup>. The Fourier method (*iii*) uses the pressure distribution in a Fourier radiation integral<sup>18,19</sup>, *e.g.* to represent the effects of turbulent shear layers<sup>20</sup> and random wall linings<sup>21</sup> on acoustic fields<sup>22,23</sup>. The Fresnel method (*iv*) uses a distribution of virtual sources<sup>24,25</sup> to represent acoustic radiation<sup>26,27</sup>. Since it is the simplest, it may be used as starting point for further elaboration.

The geometry considered here is motivated by the problem of engine noise shielding by the wing and fuselage of an airplane. Most current airliners have engines mounted in underwing nacelles, allowing direct sound radiation to the ground, besides reflection from the underside of the wing and fuselage. A pioneering aircraft design from the 70s was the VFW 614, which had the engines in overwing nacelles, which is a configuration providing shielding of engine noise. Since this aeroplane reached only prototype stage, and was not widely operated, there is little experience with such noise shielding configurations. The expansion of air transport, and tighter certification rules and airport limits on aircraft noise, lead to the reconsideration of novel aircraft configurations, featuring engine noise shielding, whose effects it is important to quantify.

The effectiveness of an engine noise shielding configuration can be specified by a shielding factor, defined as the ratio of the acoustic pressure received by the observer in the presence of shielding obstacle, and in its absence (*i.e.* in free space). The shielding factor is calculated using the Huyghens' principle, in a two-dimensional configuration (figure 3), in which the: (i) shielding is due to the wing, represented as a flat plate of chord  $c$ ; (ii) the point source  $S$  represents an overwing mounted engine, at arbitrary position relative to the wing; (iii) the observer  $O$  is at an arbitrary position below the wing. The shielding factor for this configuration is calculated, using the method of virtual sources; the plots of the amplitude and phase of the shielding factor, for a 'fly-over' observer position, show the effects of overwing engine positioning relative to the wing.

## 2 Method of virtual sources

The method of virtual sources replaces the real source of sound (figure 1a), by a distribution of virtual sources around the obstacle (figure 1b) or in a slit (figure 1c).

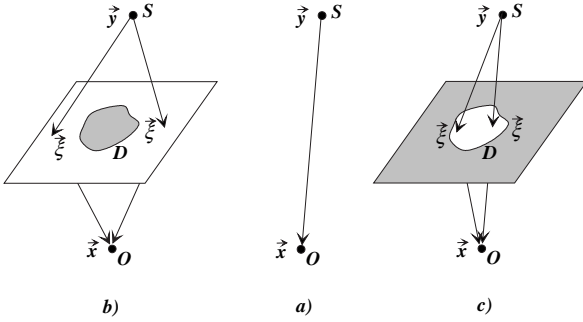


**Fig. 1** Source  $S$  radiating to observer  $O$  in free space (a), with shielding by an obstacle (b) or with the obstacle replaced by a slit in a screen (c).

### 2.1 Direct problem: shielding by an obstacle

Consider a point source of sound  $S$  at position  $\vec{y}$ , radiating to an observer  $O$  at position  $\vec{x}$ , a spheri-

cal wave, with acoustic pressure:

$$P_0(\vec{x}, t) = \{S_0/|\vec{x} - \vec{y}|\} e^{i[k|\vec{x} - \vec{y}| - \omega t]}, \quad (1)$$

where  $S_0$  is the source strength per radian,  $k$  the wave number and  $\omega$  the frequency. In what follows the factor  $S_0 e^{-i\omega t}$  is unchanged, and thus can be suppressed from now on. If an obstacle  $D$  is inserted between the source and observer (figure 1b), then the acoustic pressure at the observer is given by:

$$p_1(\vec{x}, t) \equiv F p_0(\vec{x}, t) = F |\vec{x} - \vec{y}|^{-1} e^{ik|\vec{x} - \vec{y}|}, \quad (2)$$

where, by definition  $F$  is the shielding factor. Thus the shielding factor  $F \equiv p_1/p_0$  is defined as the ratio of the acoustic pressure received at the observer in the presence  $p_1$  and absence  $p_0$  of obstacle.

In order to calculate the shielding factor effect, the method of virtual sources may be used: (i) the real (figure 1a) sound source  $S$  at position  $\vec{y}$  is replaced (figure 1b) by a distribution of virtual sources on the plane  $\vec{\xi}$  of the obstacle  $D$ , and outside the obstacle  $\tilde{D}$ , whose strength is that of a spherical wave radiated from the real to the virtual sources:

$$q(\vec{\xi}) = |\vec{\xi} - \vec{y}|^{-1} e^{ik|\vec{\xi} - \vec{y}|}; \quad (3a)$$

(ii) each virtual source re-radiates a spherical wave to the observer at position  $\vec{x}$ , leading by superposition to the acoustic field:

$$p_1(\vec{x}) = \int_{\tilde{D}} q(\vec{\xi}) |\vec{x} - \vec{\xi}|^{-1} e^{ik|\vec{x} - \vec{\xi}|} d^2\vec{\xi}. \quad (3b)$$

This method is less accurate than a Fourier method, (*i.e.*) is an approximation since it uses the same wavenumber  $k$  in (3a) and (3b).

Substitution of (3a) in (3b) specifies the acoustic field at the observer in the presence of obstacle:

$$p(\vec{x}) = \int_{\tilde{D}} e^{ik\{|\vec{\xi} - \vec{y}| + |\vec{x} - \vec{\xi}|\}} \times |\vec{\xi} - \vec{y}|^{-1} |\vec{x} - \vec{\xi}|^{-1} d^2\vec{\xi}, \quad (4)$$

or by comparison with the direct sound field (1), the shielding factor (2):

$$F(\vec{x}, \vec{y}) = e^{-ik|\vec{x}-\vec{y}|} |\vec{x}-\vec{y}| \int_{\tilde{D}} e^{ik\{|\vec{\xi}-\vec{y}|+|\vec{x}-\vec{\xi}|\}} \times |\vec{\xi}-\vec{y}|^{-1} |\vec{x}-\vec{\xi}|^{-1} d^2\vec{\xi}, \quad (5)$$

which depends on the positions of source  $\vec{y}$  and observer  $\vec{x}$ . The shielding factor is unity in free space  $F = 1$  for  $p_1 = p_0$ , *i.e.* in the absence of obstacle, and would be zero if the obstacle totally enclosed the source  $F = 0$  for  $p_1 = 0 \neq p_0$ . In most cases the modulus of the shielding factor will be between zero and one " $0 < |F| < 1$ ", representing partial noise shielding. However, the shielding factor can be greater than unity, for example, if the source and observer lie on the same side of the obstacle, which acts as a reflector; in this case the observer receives both direct ( $d$ ) and reflected ( $r_1, r_2$ ) waves, and if they are in phase, amplification  $|F| > 1$  could result. If they are out-of-phase, then attenuation  $|F| < 1$  could occur. This example shows that the shielding factor is affected by interference between the waves re-radiated by the virtual sources and thus is generally complex, implying that the introduction of an obstacle can change both the amplitude  $|F| \neq 1$  and phase  $\arg(F) \neq 0$  of sound.

## 2.2 Complementary problem: transmission through a slit

The calculation of the shielding factor (5), involves the integration of the diffraction function:

$$f(\vec{x}, \vec{y}; \vec{\xi}) = \left\{ |\vec{x}-\vec{y}| / \left( |\vec{\xi}-\vec{x}| |\vec{\xi}-\vec{y}| \right) \right\} \times \exp \left\{ ik \left( |\vec{\xi}-\vec{x}| + |\vec{\xi}-\vec{y}| - |\vec{\xi}-\vec{y}| \right) \right\}, \quad (6)$$

over the exterior  $\tilde{D}$  of the obstacle  $D$ :

$$F(\vec{x}, \vec{y}) = \int_{\tilde{D}} f(\vec{x}, \vec{y}, \vec{\xi}) d^2\vec{\xi}; \quad (7)$$

which is an infinite domain.

If instead (figure 1c) the integration is performed over the finite domain  $D$  of the obstacle:

$$G(\vec{x}, \vec{y}) = \int_D f(\vec{x}, \vec{y}, \vec{\xi}) d^2\vec{\xi}, \quad (8)$$

this specifies the slit factor  $G$ , for the complementary problem of sound transmission through a hole of shape  $D$  in an infinite rigid screen, leading to the acoustic pressure at the observer,

$$p_2(\vec{x}) \equiv Gp_0 = G|\vec{x}-\vec{y}|^{-1} e^{ik|\vec{x}-\vec{y}|}. \quad (9)$$

Thus the slit factor  $G \equiv p_2/p_0$  is defined as the ratio of the acoustic pressure received at the observer through the slit  $p_2$ , to that in free space  $p_0$  (*i.e.* without screen).

The sum of the acoustic fields transmitted through the slit  $D$  coinciding with the obstacle  $p_1$  plus that  $p_2$  transmitted through the outside of the obstacle  $\tilde{D}$ , should be the acoustic field in free space  $p_0$ , *viz.*:

$$p_0 - E = p_1 + p_2 = \iint_{-\infty}^{+\infty} f(\vec{x}, \vec{y}; \vec{\xi}) d^2\vec{\xi}, \quad (10)$$

apart from the absolute error  $E$  of the method. The latter is due to the possible difference between the acoustic field of the real source  $p_0$  and that of an infinite distribution of virtual sources over the whole  $\vec{\xi}$ -plane. Using the definitions of shielding  $F$  (2) and slit  $G$  (9) factors in (10), it follows that they are related by (11a):

$$F + G = 1 - \varepsilon, \quad \varepsilon \equiv E/p_0, \quad (11a,b)$$

where  $\varepsilon$  is the relative error of the method. If the latter is zero,  $\varepsilon = 0$ , or known, or negligible,  $\varepsilon \ll 1$ , then it is equivalent to calculate the shielding  $F$  or slit  $G$  factors, *i.e.* the direct slit problem (figure 1b) and complementary slit problem (figure 1c) are equivalent. In this case, it is easier to solve the complementary problem, because the slit factor (8) involves the same integration (8), but over a finite domain  $D$  (instead of an infinite domain  $\tilde{D}$  for (7) the shielding factor).

## 2.3 Two-dimensional approximation for a flat plate

The noise shielding configuration to be considered is an idealized version of fly-over noise from an aircraft with overwing mounted engines, further simplified in a two-dimensional configuration: (i) the wing is represented as a flat plate,

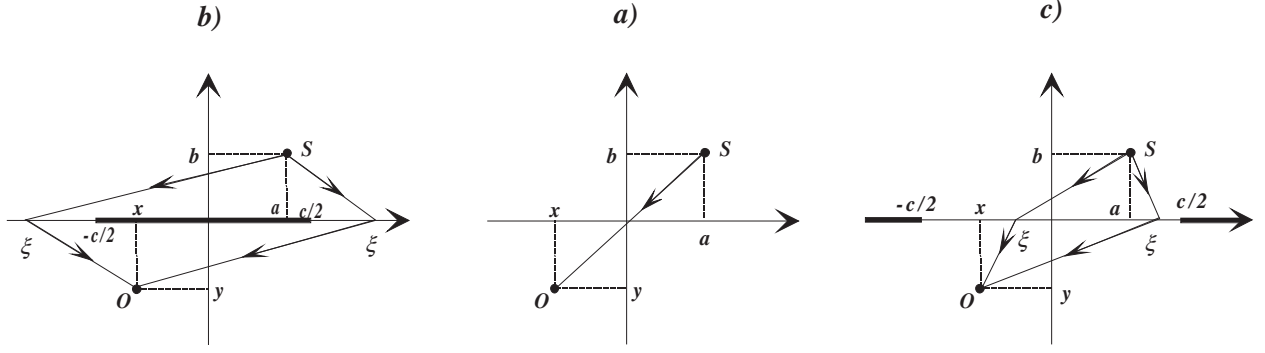


**Fig. 2** Two-dimensional configuration corresponding to figure 1, viz. source  $S$  radiating to observer  $O$  in free space (a), with shielding by a plate (b) or width (c), or through a slit (c) of width  $c$ .

of length equal to the chord  $c$ ; (ii) the engine is represented by a point source of sound  $S$ , at arbitrary position  $(a, b)$  above the wing  $a > 0$ , usually in the near field  $a \sim c \sim b$ ; (iii) the observer is at an arbitrary position  $(x, y)$  below  $y < 0$ , usually in the far-field  $-y \gg c$ . The direct spherical wave (figure 2a) from source to observer specifies the acoustic pressure in free space:

$$p_0 = e^{ikr}/r, \quad r \equiv |(x-a)^2 + (y-b)^2|^{1/2}, \quad (12a,b)$$

and also (figure 3) the virtual sources on the  $OX$ -axis:

$$q(\xi) = e^{ikr_1}/r_1, \quad r_1 \equiv |(a-\xi)^2 + b^2|^{1/2}, \quad (13a,b)$$

which are used in the direct shielding problem (figure 2b) and complementary slit problem (figure 2c).

Multiplying (13a) by the spherical waves from the virtual sources to the observer, specifies the transmission function:

$$g(\xi) = q(\xi)e^{ikr_2}/r_2, \quad (14a)$$

$$r_2 \equiv |(x-\xi)^2 + y^2|^{1/2} \quad (14b)$$

which appears in: (i) the direct problem (figure 2b) to calculate the sound field received by the observer in the presence of an obstacle:

$$p_1 = \int_{|\xi| > c/2} g(\xi) d\xi; \quad (15a)$$

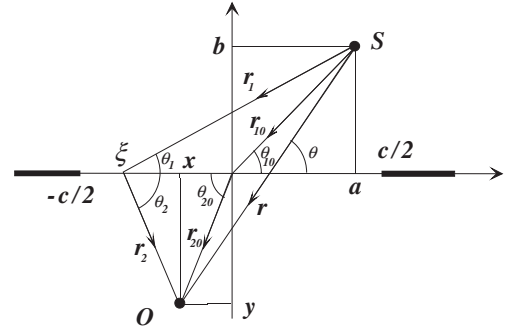


**Fig. 3** Geometrical parameters for real sound source  $S$  radiating to an observer  $O$  through a slit of width  $c$ , with virtual sound sources at  $\xi$ , distributed in the slit.

(ii) the complementary problem (figure 2c) to calculate the sound field received by the observer through the slit:

$$p_2 = \int_{-c/2}^{c/2} g(\xi) d\xi. \quad (15b)$$

In both cases the two-dimensional approximation is used, by considering only virtual sources in the  $XOY$ -plane.

The slit factor is given, using (15a, 14a, 13a, 12a) by:

$$p_2/p_0 = \int_{-c/2}^{c/2} f(\xi) d\xi = G(c), \quad (16)$$

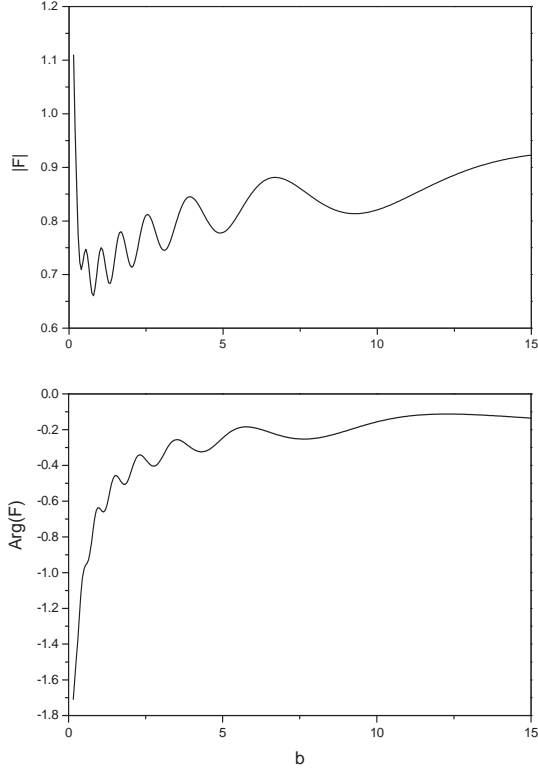


**Fig. 4** Modulus (top) and phase (bottom) of shielding factor, for sound source at mid-chord position, as a function of distance from the wing.

where  $f$  is the diffraction function:

$$\begin{aligned} f(\xi) &= re^{-ikr} g(\xi) = e^{ik(r_2-r)} r/r_2 q(\xi) \\ &= [r/(r_1 r_2)] e^{ik(r_1+r_2-r)}. \end{aligned} \quad (17)$$

The shielding factor is given by:

$$\begin{aligned} p_1/p_2 &= \int_{|\xi|>c/2} f(\xi) d\xi = \\ &= F(c) = G(\infty) - G(c). \end{aligned} \quad (18)$$

The relative error of the method (11a) is

$$\varepsilon = 1 - F(c) - G(c) = 1 - G(\infty). \quad (19)$$

Thus the method is exact  $\varepsilon = 0$ , if  $G(\infty) = 1$ , *i.e.* a distribution of virtual sources over the whole  $OX$ -axis is equivalent to the real source. In this case:

$$G(\infty) = 1 : F(c) = 1 - G(c), \quad (20)$$

the shielding factor  $F$  is one minus the slit factor  $G$ . The latter is easier to calculate, because it involves the integration (17) over the finite domain (16).

### 3 Shielding and Slit factors

The shielding, or alternatively the slit, factor, is calculated for arbitrary source and observer positions, then simplified for observer in the far-field with source in the near field, and then further simplified to observer and source both in the far field.

#### 3.1 Arbitrary source and observer positions

The slit factor is specified by the finite integral (16) over the shielding function (17), where the distance  $r_{10}$  and angle  $\theta_{10}$  of the source relative to the origin (figure 3) are used in the distance  $r_1$  from the real source to the virtual source (13b):

$$\begin{aligned} r_1 &= \left| (r_{10} \cos(\theta_{10}) - \xi)^2 + (r_{10} \sin(\theta_{10}))^2 \right|^{1/2} \\ &= \left| r_{10}^2 - 2\xi r_{10} \cos(\theta_{10}) + \xi^2 \right|^{1/2}, \end{aligned} \quad (21a)$$

and likewise the distance  $r_2$  from virtual source to observer (14b), is expressed in terms of distance  $r_{20}$  and angle  $\theta_{20}$  of observer to the origin:

$$\begin{aligned} r_2 &= \left| (r_{20} \cos(\theta_{20}) - \xi)^2 + (r_{20} \sin(\theta_{20}))^2 \right|^{1/2} \\ &= \left| r_{20}^2 - 2\xi r_{20} \cos(\theta_{20}) + \xi^2 \right|^{1/2}. \end{aligned} \quad (21b)$$

The constants:

$$r_{10} \equiv |a^2 + b^2|^{1/2}, \quad r_{20} \equiv |x^2 + y^2|^{1/2}, \quad (22a,b)$$

$$\tan(\theta_{10}) = b/a, \quad \tan(\theta_{20}) = y/x, \quad (23a,b)$$

are specified by the source ( $a, b$ ) and observer positions.

The slit factor (16, 17) is given by:

$$G(c) = re^{-ikr} \int_{-c/2}^{c/2} e^{ik(r_1+r_2)} / r_1 r_2 d\xi, \quad (24)$$

where the dependence of  $r_1, r_2$  on  $\xi$  are specified by (21a,b), for arbitrary observer and source positions. The aircraft noise problem has usually

two aspects: (i) for internal noise, the passenger may be in the near field, but is shielded by the aircraft cabin; (ii) for external noise, measured on the ground, the observer is in the far-field. On the other hand, in order for noise shielding to be effective, the engine must be close to the wing. Thus for the shielding of external noise, it is appropriate to consider the source in the near-field and the observer in the far-field.

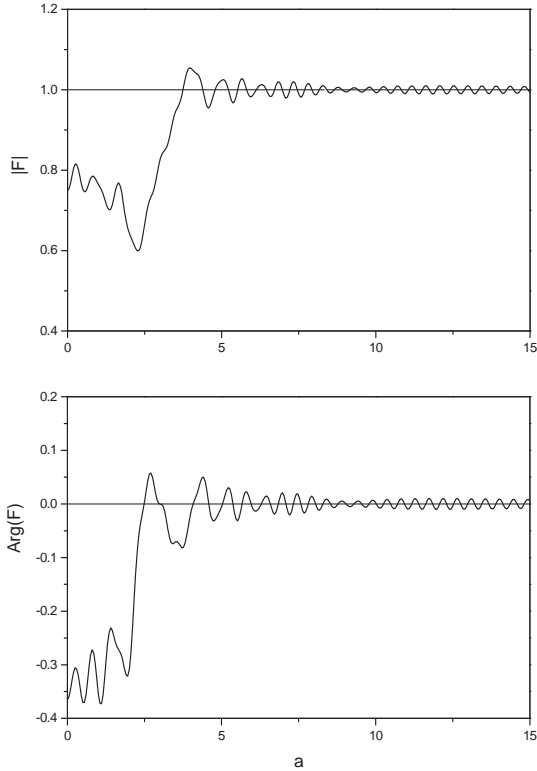


**Fig. 5** As figure 4, with sound source at a distance of one chord from the wing, as a function of distance from mid-position.

### 3.2 Near-field source and far-field observer

If it is assumed that the distance of the observer is much larger than the chord:

$$r_1 \sim c \ll r_2, r, \quad (25a)$$

$$\theta_1 - \theta_{10} \sim 1 \gg \theta_2 - \theta_{20}, \quad (25b)$$

then (21b) can be approximated:

$$r_2 = r_{20} - \xi \cos(\theta_{20}) + O(\xi^2/r_{20}), \quad (26a)$$

$$\frac{1}{r_2} = \frac{1}{r_{20}} [1 + (\xi/r_{20}) \cos(\theta_{20})] + O(\xi^2/r_{20}^3). \quad (26b)$$

Substitution of (26a,b) and (21a) specifies the slit factor (24) as:

$$G(c) = [cr/r_{10}r_{20}] e^{ik(r_{10}+r_{20}-r)} H(c), \quad (27)$$

where the coefficient is the diffraction function (17) calculated at the origin  $f(0)$ , and multiplied by the plate width  $c$  to become dimensionless; thus the dimensionless slit factor is specified by:

$$\begin{aligned} r^2, r_{20}^2 \gg r_{10}^2 : \\ H(c) = \frac{1}{c} \int_{-c/2}^{c/2} (1 + (\xi/r_{20}) \cos(\theta_{20})) \\ \times [1 - 2(\xi/r_{10}) \cos(\theta_{10}) + (\xi/r_{10})^2]^{-11/2} \\ \times \exp\{-ik[r_{10} + \xi \cos(\theta_{20}) +]\} \\ \times \exp\left\{-ik\left[(r_{10}^2 - 2\xi r_{10} \cos(\theta_{10}) + \xi^2)^{1/2}\right]\right\} d\xi, \end{aligned} \quad (28)$$

and can be simplified further in the case of source also in the far-field.

### 3.3 Source and observer both in the far-field

If the source is also in the far-field, then relations similar to (26a,b) hold also for  $r_2$ , and the dimensionless slit factor (28) simplifies to:

$$\begin{aligned} c^2 \ll r_{10}^2, r_{20}^2, r_{10}r_{20} : \\ H(c) = \frac{1}{c} \int_{-c/2}^{+c/2} \left[1 + \xi \left(\frac{\cos(\theta_{20})}{r_{20}} + \frac{\cos(\theta_{10})}{r_{10}}\right)\right] \times \\ \times \exp\{-ik\xi[\cos(\theta_{10}) + \cos(\theta_{20})]\} d\xi, \end{aligned} \quad (29)$$

which involves the dimensionless parameters:

$$\alpha \equiv (kc/2) [\cos(\theta_{10}) + \cos(\theta_{20})], \quad (30a)$$

$$\beta \equiv c [\cos(\theta_{10})/r_{10} + \cos(\theta_{20})/r_{20}]. \quad (30b)$$

Substitution of (30a) in (29) leads to:

$$\eta \equiv \xi c : H = \int_{-1/2}^{1/2} (1 + \beta\eta) e^{-2i\alpha\eta} d\eta, \quad (31)$$

which is a simple integration:

$$H = \frac{\sin(\alpha)}{\alpha} + i \frac{\beta}{2\alpha} \left( \cos(\alpha) - \frac{\sin(\alpha)}{\alpha} \right). \quad (32)$$

The dimensionless slit factor is complex, with phases and modulus:

$$\tan\{\arg(H)\} = \frac{\beta}{2} \cot(\alpha) - \frac{\beta}{2\alpha}, \quad (33a)$$

$$\alpha^2(H) = (\beta^2/4) \cos^2(\alpha) - (\beta^2/4\alpha) \sin(2\alpha) + [1 + (\beta/2\alpha)^2] \sin^2(\alpha), \quad (33b)$$

involving:

$$\beta \equiv c [\cos(\theta_{10})c/r_{10} + \cos(\theta_{20})c/r_{20}] \ll 1, \quad (34a)$$

$$\alpha \equiv (\cos(\theta_{10}) + \cos(\theta_{20}))kc/2 \sim kc/2 \sim \pi c/\lambda, \quad (34b)$$

$$\beta/2\alpha = \left( \frac{\cos(\theta_{10})}{r_{10}k} + \frac{\cos(\theta_{20})}{r_{20}k} \right) \times (\cos(\theta_{10}) + \cos(\theta_{20}))^{-1}. \quad (34c)$$

Concerning the phase of  $H$  in (33a): (i) the second term (34c) is small if the distances of observer and source from the origin are large compared with the wavelength  $kr_{10}, kr_{20} = (2\pi/\lambda)(r_{10}, r_{20}) \gg 1$ ; (ii) the first factor (34a) is also small for observer and source in the far field  $c^2 \ll r_{10}^2, r_{20}^2$ , and thus  $\arg(H)$  is small unless  $\cot(\alpha)$  is large; (iii) the latter would be the case for  $\alpha$  small in (34b), *i.e.* the wavelength is large relative to the slit width. Thus the phase of the slit/shielding factor differs significantly from that in (27)/(20) respectively, only for wavelength large compared with the width of the slit/plate. Concerning the amplitude (33b) in the same conditions of (34a,c) small, it is given approximately by the first term of (32)  $\equiv$  (35a):

$$H(c) \sim \frac{\sin(\alpha)}{\alpha}, \quad \lim_{\alpha \rightarrow 0} H(c) = 1, \quad (35a,b)$$

and thus it is unity in the case  $c/\lambda \rightarrow 0$  of wavelength much larger than the slit/plate width. The

interpretation is that in this case the slit factor may be calculated by (27) as if the virtual sources were at the origin  $H(c) = 1$ .

Using the approximation (35a) with  $\alpha$  given by (30a) in the slit function (27):

$$G(c) \sim \frac{2kr}{kr_{10}kr_{20}} e^{ik(r_{10}+r_{20}-r)} \times \frac{\sin[(kc/2)(\cos(\theta_{10}) + \cos(\theta_{20}))]}{\cos(\theta_{10}) + \cos(\theta_{20})} \quad (36)$$

it is small for observer and source in the far-field, and it simplifies in the limit of long wavelength to:

$$\lim_{kc \rightarrow 0} G(c) \sim \frac{cr}{r_{10}r_{20}} \cdot e^{ik(r_{10}+r_{20}-r)}, \quad (37)$$

and is proportional to slit width  $c$ . This result can be explained as follows: (i) for a virtual source at the origin the sound field received from the real source is  $r_{10}^{-1} e^{ikr_{10}}$  and that re-radiated to the observer is obtained multiplying by  $r_{20}^{-1} e^{ikr_{20}}$ ; (ii) since the wavelength is much larger than the slit width  $c$ , the virtual sources are approximately uniform, hence a further multiplication by  $c$ ; (iii) the slit factor is obtained by dividing by the direct wave  $r^{-1} e^{ikr}$  from real source to observer. In applications the more interesting case is that of source in the near field  $r_{10} \sim c \sim \lambda$  and wavelength comparable to the chord, when (28) specifies the slit function and (20) the shielding function, if  $G(\infty) = 1$ . The latter condition cannot be verified from (36), because the limit  $c \rightarrow \infty$  is excluded by the approximations in (29).

## 4 Amplitude and phase effects

The amplitude and phase of the shielding factor are affected by the plate compactness  $kc$  or width  $c$  on a wavelength scale (34b), and should be assessed for observer in the far-field and source in the near-field: (i) first at various vertical and transversal positions; (ii) then as carpet plots for arbitrary source positions.

### 4.1 Plate compactness on acoustic scale

The compactness parameter

$$\delta \equiv kc = 2\pi c/\lambda = 2\pi c/c_0\tau = 2\pi v c/c_0 \quad (38)$$

compares the wavelength to the plate width, and substitution in (27, 28) with  $\xi = \eta c$  and (20), yields:

$$\begin{aligned}
 1 - F &= \frac{r}{r_{20}} \frac{c}{r_{10}} e^{ik(r_{10}+r_{20}-r)} \\
 &\times \int_{-1/2}^{1/2} \{1 + \eta(c/r_{20}) \cos(\theta_{20})\} \\
 &\times [1 - 2\eta(c/r_{10}) \cos(\theta_{10}) + \eta^2(c/r_{10})^2]^{-1/2} \\
 &\times e^{-ikr_{10}[1+(c/r_{10})\eta \cos(\theta_{20})]} \\
 &\times e^{-ikr_{10}[\sqrt{1-2\eta(c/r_{10}) \cos(\theta_{10})+(\eta c/r_{10})^2}]} d\eta, \quad (39)
 \end{aligned}$$

which shows that the shielding factor depends, besides the compactness (38), only on the geometry of the problem, *viz.* through  $c/(r_{10}, r_{20}, r)$ , *i.e.*

$$F = F(kc, a/c, b/c, x/c, y/c) \quad (40)$$

the plate width  $c$  divided by the: (i) distance from observer to source  $r$ ; (ii) distance of source  $r_{10}$  and observer  $r_{20}$  from origin. For the purpose of illustration the plate width is identified with the wing chord, to which three values are given  $c = 3, 6, 9$  m; three frequencies  $\nu = 300$  Hz, 1 kHz, 3 kHz are considered, with the period  $\tau = 1/\nu$  and wavelength  $\lambda = c_0\tau$  calculated for a sound speed  $c_0 = 340$  m/s leading to the range of values of the compactness parameter shown in table 1.

$\nu$ (kHz)	$\lambda$ (m)	$c = 3$ m	$c = 6$ m	$c = 9$ m
0.3	1.13	16.6	33.3	49.9
1	0.340	55.4	111	166
3	0.113	166	333	499

**Table 1** Compactness parameters for several wave frequencies and plate widths.

Thus the plots of the shielding factor are given for:

$$c = 6 \text{ m}, \nu = 900 \text{ Hz}, \delta = 99.792 \quad (41a,b,c)$$

The observer is placed directly below the centerline, at a distance of 15 chords, corresponding to

fly-over noise:

$$x = 0 \text{ m}, y = -15c = -90 \text{ m}. \quad (42a,b)$$

For the first plot the sound source is placed at the mid-position and its distance to the plate varied between 0.05 and 2.5 chords:

$$a = 0, 0.3 \text{ m} = 0.05c \leq b \leq 2.5c = 15 \text{ m}; \quad (43a,b)$$

for the second plot the source is kept at a distance of one chord from the plate, and moved parallel to the plate up to 2.5 chord lengths:

$$b = c = 3 \text{ m}, 0 \text{ m} = 0.0c \leq a \leq 2.5c = 15 \text{ m}. \quad (44a,b)$$

The shielding factor  $F$  is plotted respectively in figure 4 and 5, with the modulus  $|F|$  at the top and the phase  $\arg(F)$  below.

## 4.2 Vertical and horizontal displacement of the source

From the figure 4 top it is clear that some shielding effect is present even with the source on the centerline position two-and-a-half chords away, since  $|F| \sim 0.9$  for  $b = 2.5c$ . The shielding effect does not go beyond  $|F| = 0.66$  when the source is close to the plate  $b \sim 0.1c$ . The amplitude of the shielding factor is oscillatory, as a consequence of wave interference. Thus  $|F|$  can vary between  $0.66 < |F| < 0.78$  over a small range of distances  $0.05c < b < 0.3c$ , depending on whether wave interference is destructive or constructive, and leads to maxima or minima. Thus small displacements of the source near the obstacle can lead to different values of the shielding factor. The same applies to frequency changes, so that a good shielding for one frequency can degrade for another frequency. Farther from the obstacle, the maxima and minima are more spaced; thus the shielding factor is less sensitive to small changes in the position and frequency of the source. However, in this case the shielding effect is also weaker. The phase of the shielding factor (figure 4, bottom) does not change by more than  $-0.3\pi$  if the source is more than one chord away from the plate. Significant phase changes occur

only when the source is within one width of the plate, and they increase rapidly when the source approaches the plate. The phase has oscillations, due to wave interference effects. These are more visible not too close to the plate  $0.3c \leq b \leq c$ . The maxima and minima become more spaced farther from the obstacle, when the phase effect is smaller.

If the sound source is displaced vertically, the plate remains as an obstacle in the direction of the observer, and thus some shielding effect is observed in figure 4, even for distances larger than a chord. If the sound source is displaced horizontally, then it comes into direct radiation line-of-sight to the observer beyond half-chord  $a > c/2 > 3$  m, and the shielding effect ceases in figure 5. It can be confirmed in figure 5 that when the sound source comes in line-of-sight of the observer, the amplitude of the shielding factor (top) tends to unity  $|F| = 1$  at the top and the phase to zero  $\arg(F) = 0$  at the bottom for  $-a > c/2 = 3$  m, but there are oscillations, due to the edge effect of the plate, as for Fresnel diffraction<sup>25</sup>. These oscillations die out slowly as the line-of-sight from source to observer is further displaced away from the edge of the plate. It is more interesting to see that the modulus of the shielding factor can be as low as  $F = 0.6$ , if the sound source lies behind the plate, somewhat offset at  $a = 2.2$  m =  $0.73c$ . Moving the sound source to the centerline degrades the shielding effect to  $F = 0.75$  at  $a = 0.0$  m =  $0.0c$ . When the source is behind the plate  $b < 3$  m =  $c/2$  both the modulus (top) and phase (bottom) of the shielding factor have oscillations due to wave interference effects.

### 4.3 Carpet plots of modulus of shielding factor

In order to check in general the effect of source position relative to the obstacle, it is necessary to make a two-dimensional plot of the modulus of the shielding factor (figure 6). The latter shows that to maximize the noise shielding effect, the sound source: (i) should be less than half-chord away from the wing, but need not be much

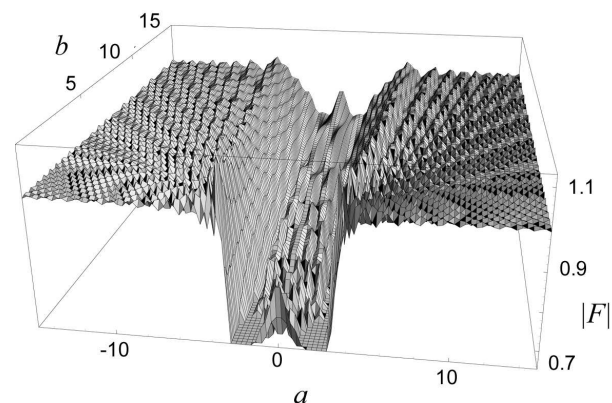


**Fig. 6** Plot showing the modulus of the shielding factor, depending on source position relative to the plate (*i.e.* engine position relative to the wing).

closer; (ii) should not be neither ahead or behind the wing and the center is not the best position, but rather the optimum position is offset at about one-quarter or three-quarters chord. These two results are compatible with other design requirements: (i) the nacelle diameter excludes an engine too close to the wing; (ii) the aerodynamics of the air intake and exhaust may benefit from a choice of a relatively forward quarter-chord engine position.

For an observer at mid-position, a source at mid-position is not the best shielding solution, because the configuration (figure 7a) is ‘too symmetrical’: (i) the sound paths 1 and 2 around the plate are longer than the direct sound path 0 without the plate, and the spherical decay of amplitude, implies a noise reduction; (ii) since the paths 1 and 2 are symmetrical, the waves arrive in phase, and reinforce each other. If the source is shifted away (figure 7b) from the centerline position, the ‘symmetry’ is broken, and the paths 1 and 2 are of unequal length, so that there can be phase interference in addition to amplitude decay, leading to a stronger shielding effect. The off-set of the source from centerline position which gives the strongest shielding will depend on the ratio of the wavelength of sound to the wing chord.

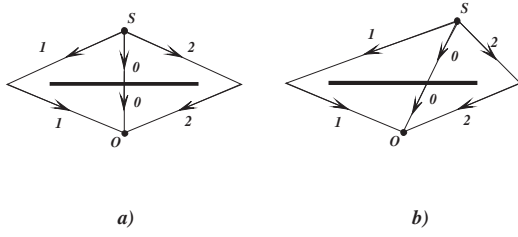


**Fig. 7** Point–source  $S$  at symmetrical (a) and un-symmetrical (b) positions.

## 5 Discussion

The choice of parameters for the problem, *i.e.* relative positions of sound source and wing is reviewed over the audible range, before discussing again the carpet plots for the shielding factor for several wavelengths larger than, comparable to or smaller than the chord. The effect on the amplitude and phase of the shielding factor, of interference between two sources, is also considered.

### 5.1 Shielding factor over the audible frequency range

The ‘four frequencies’ considered in table 1 correspond to the part 0.3 – 3 kHz of the audible spectrum 20 Hz – 20 kHz of most concern to aircraft noise. In order to scan more fully the range of values of the shielding factor: (i) the observer position is retained in the fly-over direction 15 chords away  $x = 0$  and  $y/c = -15$  as in (42a,b); (ii) the source position relative to the wing is varied in the same ranges  $0 \leq a/c \leq 2.5$  in (44b) horizontally and  $0.05 \leq b/c \leq 2.5$  vertically; (iii) the remaining dimensionless parameter is the compactness (42) or ratio of wavelength to chord, which is given the values

$$2\pi/\delta = \lambda/c = 6, 1, 0.6, 0.3, 0.1, 0.02. \quad (45)$$

In order to justify this choice of values we start with the same wavelength of sound over the audible range for a sound speed  $c_0 = 340$  m/s in the international standard atmosphere at sea level. The mean chord  $\bar{c} = S/\bar{b}$ , which is the ratio of

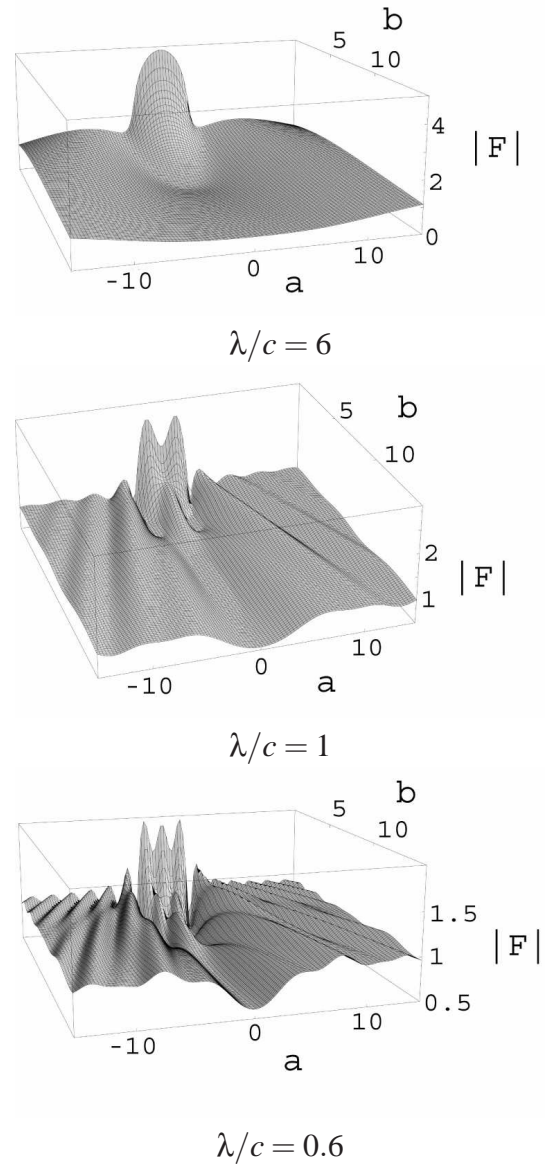


**Fig. 8** Shielding factor for wavelength comparable to or larger than the chord.

wing area  $S$  to span  $\bar{b}$ , is given for the most widely used current airliners<sup>28</sup> in table 3.

These aircraft have swept wings, whereas the present model considers rectangular wings.

The data serves as indication that it is sufficient to consider a range of wing chords  $c = 3, 6, 9$  m in table 3 together with the wavelengths  $\lambda$  in table 2, to arrive at the ratio in table 4. The ratio of wavelength of sound to wing chord lies in the range  $0.002 \leq \lambda/c < 5.667$ , and is covered by the choices in (41).

frequency ( $f$ ) Hz	wavelength ( $\lambda$ ) m
20	17
500	0.68
$10^3$	0.34
$2 \times 10^3$	0.17
$10^4$	0.034
$2 \times 10^4$	0.017

Table 2 Audible wavelength of sound.

Model	Wing		
	Area $S$ $m^2$	Span $\bar{b}$ m	Mean chord m
B737-700	125.00	34.31	3.64
B747-400	541.16	64.44	8.40
B757-200	185.25	38.05	4.87
B767-300	283.30	47.57	5.96
B777-100	427.80	60.93	7.02
A300-600	260.00	44.84	5.80
A310-300	219.00	43.90	4.99
A320	122.60	34.09	3.60
A340-200	361.60	60.30	6.00

Table 3 Wing data of current Jet Airliners.

### 5.2 Effect of ratio of wavelength of sound to wing chord

The first set of three carpet plots in figure 8 correspond to the three long wavelengths  $\lambda/c = 6, 1, 0.6$  and are seen ‘from the back’ to improve visibility. For the longest wavelength (figure 8, top) the shielding factor is about unity, implying that the small plate cannot ‘shield’ the long waves; however, the shielding factor becomes large (up to  $|F| = 4$ ) just behind the plate  $b/c \ll 1$ ,  $a/c \sim 0$ , because of the positive interference of waves in a symmetrical source position (figure 7a); as  $|a/c|$  increases, and the source position becomes unsymmetrical (figure 7b), this positive interference reduces. In the case of wavelength equal to chord  $\lambda = c$  in figure 8b, there is a smaller positive interference peak  $|F|_{max} = 2.6$ , which reduces further  $|F|_{max} = 1.8$  for wave-

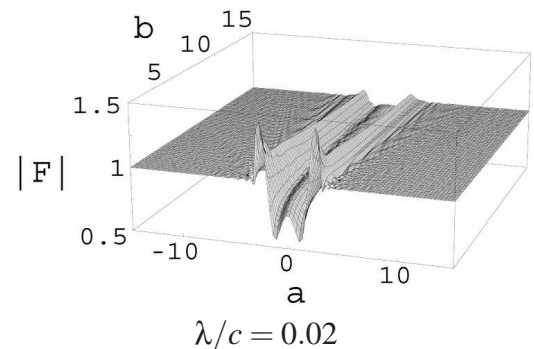
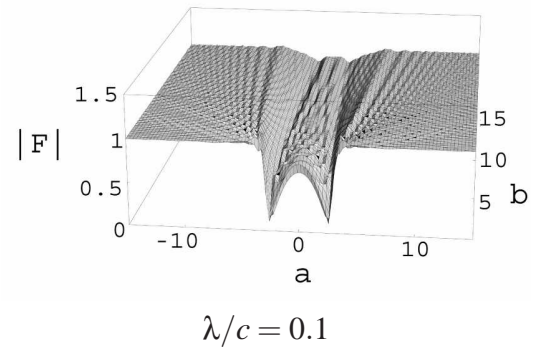
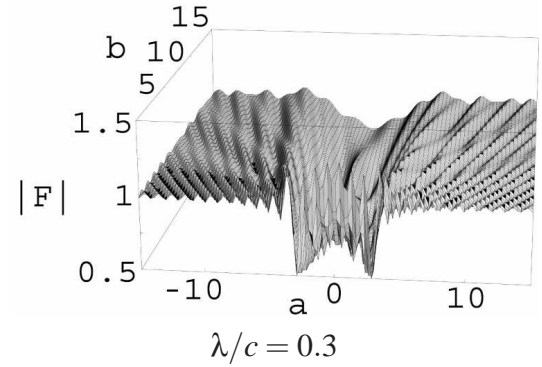


Fig. 9 Shielding factor for wavelength much smaller than the chord.

length shorter than the chord  $\lambda = 0.6c$  in figure 8c. The plots in figure 8 remind that the shielding factor can be locally greater than unity, due to positive interference; the table 4 shows that this case of wavelengths comparable to or larger than the chord, occurs only for smaller airliners and frequencies close to the lower audible limit.

The more typical situation for aircraft noise is that in figure 9, of wavelength smaller than the chord, for which the shielding factor is also close to unity outside the plate, and behind it, the peaks above  $|F| = 1$  for  $\lambda = 0.3c$  in figure 9c, re-

Sound frequency	Wing Chord c(m)		
	3	6	9
20 Hz	5.667	2.873	1.889
500 Hz	0.227	0.113	0.076
1 kHz	0.113	0.057	0.038
2 kHz	0.057	0.011	0.019
10 kHz	0.011	0.006	0.004
20 kHz	0.006	0.003	0.002

**Table 4** Wing data of current Jet Airlines.

cede to  $|F| < 1$  at all points behind the plate for  $\lambda = 0.1c$ . Even for  $\lambda = 0.02c$  in figure 9c, which corresponds to ray theory, the shielding factor  $|F| < 1$  remains significantly different from zero, in the symmetric source position and the phenomenon of ‘edge diffraction’ becomes apparent: the shielding factor exceeds unit in a narrow region near the edges of the plate, at the transition between the ‘sound zone’ and ‘zone of silence’ (which corresponds to the transition light-shadow in optics). A small shielding factor  $|F| < 0.1$  can be obtained for an unsymmetrical position behind the wing.

## References

- <sup>1</sup>A. Sommerfeld (1960). *Optics*, Academic Press.
- <sup>2</sup>A. Sommerfeld (1896). Mathematik Theorie der Diffraction (Mathematical Theory of Diffraction), *Math. Ann.* **68**, 317.
- <sup>3</sup>B. Noble (1958). *The Wiener-Hopf technique*, Oxford U.P.
- <sup>4</sup>D. S. Jones (1978). Acoustics of a splitter plate, *J. Inst. Math. Appl.* **21**, 197-209.
- <sup>5</sup>D. S. Jones (1986). Diffraction by three semi-infinite planes, *Proc. Roy. Soc.* **A404**, 299-321.
- <sup>6</sup>D. G. Crighton & F. G. Leppington (1973). Singular perturbation methods in acoustics: diffraction by a plate of finite thickness, *Proc. Roy. Soc.* **A335**, 313-339.
- <sup>7</sup>J. D. Achenbach & Z. L. Li (1986). Reflection and transmission of scalar waves by a periodic array, *Wave Motion* **8**, 225-234.
- <sup>8</sup>W. H. Lin & A. C. Raptis (1986). Sound Scattering from a thin rod in a viscous medium, *J. Acoust. Soc. Am.* **79**, 1693-1701.
- <sup>9</sup>P. F. Hummelgens (1980). Axial Scattering of sound by a torus, *Acustica* **44**, 62-67.
- <sup>10</sup>J. W. S. Rayleigh (1877). *Theory of Sound*, 2 Vols, Dover.
- <sup>11</sup>M. J. Lighthill (1978). *Waves in fluids*, Cambridge U. P.
- <sup>12</sup>L. M. B. C. Campos & P. G. T. A. Serrão (2004). On the acoustics matching of straight, curved and twisted ducts (to appear).
- <sup>13</sup>M. S. Howe (1976). The attenuation of sound by a randomly irregular impedance layer, *Proc. Roy. Soc.* **347**, 513-535.
- <sup>14</sup>L. M. B. C. Campos (1978). On the Spectral broadening of sound by turbulent shear layers. Part I: Scattering by moving interfaces and refraction in turbulence, *J. Fluid Mech.* **89**, 723-749.
- <sup>15</sup>L. M. B. C. Campos (1986). On waves in gases. Part I: Acoustics of jets, turbulence and ducts, *Rev. Mod. Phys.* **58**, 117-192.
- <sup>16</sup>M. S. Howe (1973). On the kinetic theory of wave propagation in random media, *Phil. Trans. Roy. Soc.* **A274**, 523-549.
- <sup>17</sup>L. M. B. C. Campos (1992). Effects on acoustic fatigue loads of multiple reflections between a plate and a turbulent wake, *Acust.* **76**, 109-117.

<sup>18</sup>P. M. Morse & H. Feshbach (1968). *Theoretical Acoustics*, McGraw-Hill.

<sup>19</sup>A. Pierce (1981). *Acoustics*, McGraw-Hill.

<sup>20</sup>L. M. B. C. Campos (1978). On the Spectral broadening of sound by turbulent shear layers. Part II: The Spectral broadening of sound and aircraft noise, *J. Fluid Mech.* **89**, 751-783.

<sup>21</sup>M. S. Howe (1983). The attenuation of sound in a randomly lined duct, *J. Sound Vib.* **87**, 83-103.

<sup>22</sup>L. M. B. C. Campos (1995). On the correlation of acoustic pressures induced by a turbulent wake on a nearby wall, *Acustica* **82**, 9-17.

<sup>23</sup>L. M. B. C. Campos (1997). On the spectra of aerodynamic noise and aeroacoustic fatigue, *Progr. Aerosp. Sci.* **33**, 353-389.

<sup>24</sup>M. Born & E. Wolf (1959). *Principles of Optics*, Pergamon.

<sup>25</sup>L. D. Landau & E. F. Lifshitz (1966). *Theory of Fields*, Pergamon.

<sup>26</sup>J. H. Rindel (1986). attenuation of sound reflections due to diffraction, *Nordic Acoust. Meet.*, Aalborg Univ. Press, 257-260.

<sup>27</sup>L. Cremer (1990). Fresnel Methoden zur Berechnung von Beugungsfeldern, *Acustica* **72**, 1-6.

<sup>28</sup>P. Jackson (2000). *Jane's All-the-World's Aircraft*, MacDonaldis and Jane's.